# 1

# Introduction

## 1.1 Overview of Polymer Foams

Foam materials, characterized by highly porous structures, are prevalent in both natural and synthetic forms [1]. Examples in nature include natural sponges with open cellular structures and wood, which humans have used for millennia. Polymer foams are defined as a kind of polymer material formed by a large number of microcellular cells containing a gas medium uniformly dispersed in the polymer matrix. Almost all polymers can be made into polymer foams. In the twentieth century, with the growth of the polymer industry, various types of polymer foam products emerged. The introduction of the gas phase makes polymer foams possess excellent performance in material weight reduction, heat insulation, sound absorption and noise reduction, shock absorption, etc. As a gas phase and solid phase mixed material, polymer foams possess special properties. It is widely used to prepare various packaging materials, automotive and aircraft parts, sports equipment, building materials, etc.

Traditional polymer foams are mainly prepared by direct mixing of molten polymer and gas. The foams usually have large cell diameters and low cell density, and the average cell size is generally larger than 100 μm. These large cells often become the starting point of cracks, which become one of the factors restricting the performance improvement of traditional polymer foams.

With the continuous development of human society and the enhancement of people's pursuit of a higher quality of life, the performance of traditional polymer foams has gradually entered a bottleneck that cannot meet the new requirements in the fields of automobile, aircraft, aerospace, electronic devices, and medical devices. To address this problem, Professor N P Suh from MIT and colleagues first proposed the microcellular foaming technology and defined the cell size and density range. The average cell size and cell density in modern microcellular foam are in the range of 0.1–100 μm and within $10^9$–$10^{15}$ cells $cm^{-3}$. The microsized cells in the foamed part could blunt the crack tip and block the crack propagation when the cell size is smaller than the crack size, which greatly improves the mechanical properties of the polymer foams compared with traditional large cell foams [2].

Microcellular foaming enhances mechanical properties compared to traditional foams, offering more than fivefold improvements in impact strength, toughness, and fatigue life, with density reductions ranging from 5% to 95% [3].

*Functional Polymer Foams: Green Fabrication Methods, Performance and Applications*,
First Edition. Haoyang Mi.

In addition, microcellular foaming leads to lower dielectric constants and thermal conductivities [4] expanding its range of applications. Owing to their low density and high toughness, robust shock strength, and fatigue resistance, these materials are suitable for packaging, as well as shock-absorbing buffers.

In applications requiring lightweight and high-strength soundproofing, such as aircraft and automobiles, microcellular foams are preferred due to their high specific strength and effective soundproofing. Their low dielectric constant, thermal conductivity, and excellent electromagnetic shielding/absorption properties, arising from their unique vesicular structure, make microcellular foams desirable for aerospace and electronics industries. Moreover, adjusting foaming process conditions, such as temperature and pressure, allows for control over the final material structure and properties.

Beyond these properties, microcellular foams with high open porosity find applications in various fields, including biological tissue scaffolds, filtration adsorption, catalyst carriers, and sustained drug release. Traditional chemical blowing agents, like chlorofluorocarbons (CFCs) and hydrochlorofluorocarbons (HCFCs), have environmental limitations due to the emission of chlorinated pollutants. In contrast, microcellular foaming with supercritical $CO_2$ as the foaming agent is environmentally friendly and offers excellent performance making it highly promising for various applications. To delve into the advanced applications of polymer foams, it is crucial to first grasp the fundamental principles of polymer foaming technology.

## 1.2 Polymer Foaming Methods

The basic process in polymer foaming contains the blending of a polymer matrix with a foaming agent, separating gas from the polymer, and fixing the polymer matrix to form a unique uniform cellular structure. According to the gas introduction methods, polymer foaming can be roughly divided into three categories, namely, mechanical foaming, physical foaming, and chemical foaming.

### 1.2.1 Mechanical Foaming

Mechanical foaming is a method in which air is sucked into the polymer matrix by intense mechanical agitation to form a uniform foam body. Air and emulsifier or surfactant can be added to shorten the molding cycle. It is not necessary to add a foaming agent, but it has the disadvantage that the bubbles generated by this process are easy to disappear, and it is difficult to meet the production requirements of microcellular foam.

### 1.2.2 Physical Foaming

Physical foaming refers to the process in which gas is directly injected into a polymer melt to create a cellular structure. There are typically three approaches utilized:

(1) Inert gas is dissolved into a plastic melt or paste under pressure, then the pressure is released quickly, resulting in the creation of cells within the polymer matrix.
(2) Low-boiling temperature liquids that are dissolved in the polymer melt and are then evaporated at elevated temperature to form gas bubbles in the polymer matrix;
(3) Hollow microspheres or expandable microspheres are directly added to the polymer matrix via melt blending to form a porous foam structure.

In the process of physical foaming, the physical foaming agent undergoes only a change in state, such as from a saturated solution to liquid/gas, or a supercritical fluid (SCF) state to a gas, and the composition of the gas does not change. Physical foaming agents typically can be divided into two categories, namely, inorganic foaming agents and organic foaming agents. Inorganic foaming agents include $CO_2$, $N_2$, air, etc., while organic foaming agents include hydrocarbons, chlorinated hydrocarbons, fluorinated and chlorinated hydrocarbons, etc. However, due to potential environmental pollution and safety issues associated with the chemical foaming agent, such as flammability, explosiveness, and ozone depletion, most of them have been phased out or restricted for use, as people have become more aware of safety and environmental protection.

The physical foaming method using physical foaming agents has a relatively low cost, especially for $CO_2$ and $N_2$, which are inexpensive and nonpolluting. They are also flame retardant, making them highly valuable. However, it usually requires special molding machines and auxiliary equipment, and inert gases such as $CO_2$ and $N_2$ require high pressures to achieve foaming, making the process highly technically challenging and equipment demanding.

SCF foaming technology is a physical foaming method using SCF as the foaming agent. SCF refers to fluids in their supercritical state where both the temperature and pressure exceed their critical points (Figure 1.1) [6]. SCF is in the state between liquid and gas, with viscosities and diffusion coefficients close to gases and densities and solvation capabilities close to liquids. It has the advantages of both liquid and gas, such as good fluidity, large mass transfer coefficient, easy adjustment of fluid density, good diffusivity, and solubility [7]. The most commonly used SCFs are $CO_2$, $N_2$, water, ethane, etc. As listed in Table 1.1, the critical point of $CO_2$ is the temperature above 31.1 °C and pressure above 7.38 MPa, which is relatively easy to reach

**Table 1.1** Critical points of common supercritical fluids.

| Supercritical fluid | Critical temperature (°C) | Critical pressure (MPa) |
|---|---|---|
| $scCO_2$ | 31.1 | 7.38 |
| $ScN_2$ | −147.1 | 3.39 |
| $scH_2O$ | 374.2 | 21.83 |
| $ScC_2H_6$ | 32.3 | 4.82 |

Source: Adapted from Cha [8].

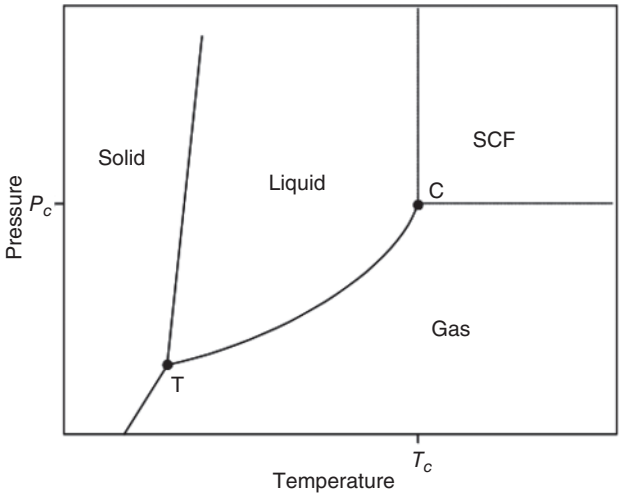


**Figure 1.1** Phase diagram of fluid: T, triple point; C critical point. Source: Nalawade et al. [5]/with permission of Elsevier.

compared with other gas/liquid [5]. In addition, attributing to the high solubility and high diffusion rate of supercritical $CO_2$ ($scCO_2$), physical foaming using $scCO_2$ as the foaming agent could achieve a higher gas content, greater expansion ratio, and higher cell density. Considering the advantages of SCF foaming using $scCO_2$ and $scN_2$, it has been widely researched in recent years and employed in the production of various thermoplastic polymer products.

### 1.2.3 Chemical Foaming

The chemical foaming method relies on chemical reactions to generate gases to form cells in the polymer matrix. Gases are typically generated by the decomposition reaction via the heating of a chemical foaming agent added to a polymer matrix. At present, common chemical foaming agents mainly include sodium bicarbonate, ammonium nitrate, azo compounds, sulfonyl hydrazides, and nitroso compounds, etc. In the chemical foaming of materials like polyurethane, gas is generated by the cross-linking reaction between the isocyanate functional groups and water molecules. For chemical foaming, the temperature and gas content of the reaction is the key to determining the foaming quality, the reaction temperature at the time of gas generation should match the processing temperature of the polymer, the rate of gas generation needs to be controllable, and the gas content needs to be adequate.

The main advantage of the chemical foaming agent is that it does not require any modification of existing plastic processing equipment, and the process of injection molding/extrusion of polymer foams using a chemical foaming agent is essentially the same as the general injection molding/extrusion process. The heating, mixing, plasticization, and most of the foaming expansion of the plastics were done in an injection molding machine/extruder. Compared to physical foaming agents,

the disadvantages of chemical foaming are mainly that they are more demanding for the reaction conditions, the foaming agents usually cost more, the potential environmental pollution, and the volatile organic compound (VOC) emission.

## 1.3 Fundamentals of SCF Foaming

In the polymer foaming process, a homogeneous system of polymer/gas solution is obtained by blending dissolution or saturation of a two-phase system consisting of polymer and gas, and then the equilibrium state of the system is broken by changing the external conditions (usually pressure and temperature) to trigger the nucleation of the cells due to the separation of the gas phase from the polymer phase owing to the transfer of the gas from the supercritical state to the gas state. Thus, the cells are the product of this phase separation process. The formed cells can, therefore, be seen as a way to counteract changes in external conditions [9], while the first half of the foaming process can be seen as a transition from a stable (homogeneous) state to a metastable or unstable (multiphase) state.

However, it is crucial to recognize that the cells formed within this metastable state lack stability due to the high molecular mobility inherent to the polymer matrix. Consequently, a reinforcement treatment, such as cooling, applied to the polymer-dense phase surrounding the cells is imperative. This treatment serves to immobilize the advantageous structure acquired during the foaming process, ultimately leading to the attainment of a stable foaming product. The latter half of the foaming process can thus be construed as a transformation of unstable foaming products into stable ones.

From the foregoing exposition, it becomes evident that the polymer foaming process is an intricate thermodynamic and kinetic undertaking. The fundamental process can be broadly delineated into five stages, as depicted in Figure 1.2 [10].

### 1.3.1 Preparation of Homogeneous Solution

A homogenous solution needs to be constructed as the basis for the physical foaming process. During the formation of gas polymer homogeneous systems, the solubility

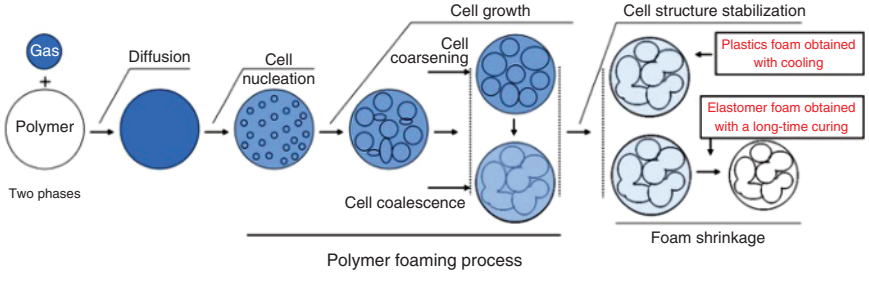


**Figure 1.2** Schematic illustration of the five stages in the SCF foaming process. Source: Zhai et al. [6]/with permission of Taylor & Francis.

of the gas is one of the most important parameters deciding the content of the foaming agent that can be introduced to the system, which in turn affects the final foam density and cell size. Determining the solubility of the foaming agent in the polymer is fundamental to the overall subsequent foaming process, so understanding the interaction between gases and the polymer melt and the influencing factors on solubility is critical.

Binary systems of gases/polymers are usually described using Henry's law, and the solubility of gases in polymers can be derived from Henry's law [11]

$$C = K_H P \tag{1.1}$$

where $C$ is the gas solubility, $K_H$ is Henry's constant, and $P$ is the gas pressure.

Thus, increasing pressure is an effective mean to enhance gas solubility, and of course, a similar effect is obtained by lowering temperature. Henry's law combined with van't Hoff equation can explain the relationship between temperature and gas solubility [12].

$$K_H = K_0 \exp\left(\frac{-\Delta H_S}{RT}\right) \tag{1.2}$$

where $K_H$ is Henry's constant, $K_0$ is pre-exponential factor, $\Delta H_S$ is the heat of the solution, $R$ is the gas constant and $T$ is temperature.

Henry's equation is based on ideal dilute solution solvent conditions without considering the interaction between gas and polymer melt, especially under high-pressure conditions, where the interaction between SCF and the polymer is more complicated. When a large amount of SCF is dissolved in the polymer, the plasticizing effect would affect the surface tension and rheological properties of the system.

The Flory Huggins equation [9] is a good guideline to determine the amount of gas used in a system, and it is expressed as:

$$\Delta F_m = kT(n_g \ln \varphi_g + n_p \ln \varphi_p + \chi n_g \varphi_g) \tag{1.3}$$

$$\chi = 0.3 + V_g/RT(\delta_p - \delta_g)^2 \tag{1.4}$$

The left-hand side of Eq. (1.3) $\Delta F_m$ refers to the mixing of free energy after the mixing of polymer and gas. On the right-hand side of the equation, $n_g$ and $\varphi_g$ refer to the moles and volume fraction of the gas, while $n_p$ and $\Phi_p$ refer to the moles and volume fractions of the macromolecules, $\chi$ is a parameter to describe the action of macromolecules and gases (consists of both entropic and enthalpic components, with an average value of about 0.3 for an entropic component of most polymer/gas systems, and the enthalpic component is determined by the solubility parameter [10]), $K$ is the Boltzmann constant, and $T$ is the thermodynamic temperature. $V_g$ in Eq. (1.4) represents the molar volume of the gas, $R$ is the ideal gas constant, and $\delta$ is the solubility parameter.

In practice, solubility is greatly affected by the temperature, pressure, and crystallization behavior of polymers [13]. Normally, the solubility of liquid/gas in a polymer matrix would increase with the increase of pressure, while decrease as the increase of temperature [14].

### 1.3.2 Cell Nucleation

The basic theory of cell nucleation in polymer foaming originates from the classical nucleation theory established by Gibbs in the twentieth century. Colton and Suh [15] described the nucleation process during foaming. The formation of cells is actually a phase separation process initiated by the rapid pressure change or temperature change. The cell nucleation step is driven by the thermodynamic instability of gas/polymer homogeneous systems under high-temperature and high-pressure conditions. The physical foaming method caused a sharp decrease in the gas solubility in the polymer by a rapid pressure drop to form very high supersaturations. When the unstable high-energy state gas molecules cross the free energy barrier, high-energy state molecules would aggregate with each other through the activation transition, and then stable nuclei are formed on these aggregation sites.

In the phase separation process, the nucleation of gas cells needs to overcome the phase transition energy barrier (i.e., the phase transition activation energy), the dynamic source of the phase transition being the difference between the free energy of the system's initial state and the end state. There are typically two types of cell nucleation mechanisms according to the difference in the initial state of the nucleation system, namely, homogeneous nucleation and heterogeneous nucleation (Figure 1.3).

#### 1.3.2.1 Homogeneous Foam Nucleation

When the system is composed of a single homogeneous phase of gas/polymer mixture, it is assumed that there are no impurities within the system that can induce nucleation. At this point, each gas molecule is a theoretical nucleation point. In a thermodynamic system composed of a polymer melt and dissolved gas, the total Gibbs free energy of the system changes according to the law of thermodynamic energy conservation $\Delta G$ consists of three parts: the change in bulk free energy, the change in chemical potential, and the change in interfacial free energy, as shown in Eq. (1.5).

$$\Delta G = -\Delta P \cdot V_G + n_g(\mu_G - \mu_L) + \gamma_{LG} \cdot A_b \tag{1.5}$$

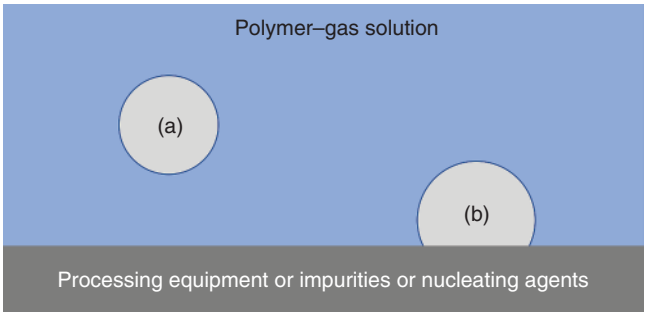


**Figure 1.3** Two nucleation types in a polymer–gas system (a) homogeneous nucleation, and (b) heterogeneous nucleation.

where $\Delta P$ is the pressure difference between inside and outside bubbles, $\mu_L$ is the chemical potential of gas molecules in polymer melts, $\mu_G$ is the chemical potential of gas molecules in bubbles, $n_g$ is the number of gas molecules in the gas phase, $A_b$ is the surface area of the bubble, and $\gamma_{LG}$ is the gas/liquid interfacial tension.

The first term is the work done by the volume expansion of the gas inside the cells, the second term is the difference in chemical potentials before and after nucleation, and the third term is the work required to create the liquid gas interface. Since the chemical potential difference is zero for the nucleus in chemical thermal equilibrium [15a], and the cell is assumed spherical for homogeneous nucleation, Eq. (1.5) can be written as:

$$\Delta G = -\frac{4}{3}\pi r^3 \cdot \Delta P + 4\pi r^2 \cdot \sigma \tag{1.6}$$

where $r$ is the cell radius and $\sigma$ is the surface tension of the polymer matrix.

The function curve of the free energy barrier $\Delta G$ and the radius $r$ of the cell nucleus during homogeneous nucleation can be obtained, and the maximum value of a $\Delta G$ corresponding to the radius size of $R_c$ can be obtained from Figure 1.4.

Since the thermodynamic system tends to maintain a low-energy state, the cell nucleus tends to collapse when the radius is smaller than $R_c$, while it can spontaneously grow up when the radius is larger than $R_c$ seeking to balance Eq. (1.7) to 0.

$$\frac{d\Delta G}{dr} = 0 \tag{1.7}$$

The formula for the critical radius $R_c$ can be derived:

$$R_c = \frac{2\sigma}{\Delta P} \tag{1.8}$$

Substituting Eq. (1.8) into Eq. (1.7) yields a uniform nucleation free energy barrier of:

$$\Delta G^*_{hom} = W_{hom} = \frac{16\pi\sigma^3}{3\Delta P^2} \tag{1.9}$$

According to the classical nucleation theory, the formula of homogeneous cell nucleation rate can be derived [15c]:

$$N_{hom} = f_0 C_0 \exp\left(\frac{-\Delta G^*_{hom}}{kT}\right) \tag{1.10}$$

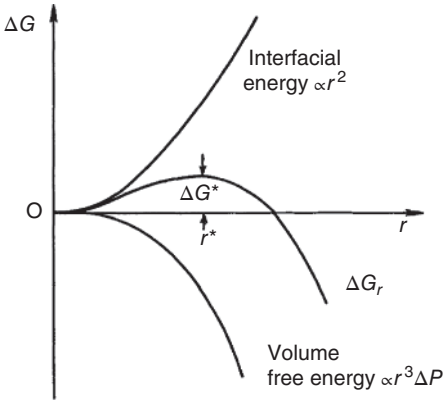


**Figure 1.4** Relationship between the free energy barrier and cell radius in homogenous nucleation. Source: Colton and Suh [15a]/with permission of John Wiley & Sons.

where $f_0$ is the frequency factor of gas molecules entering the cell nucleus, expressed in 1/s, $C_0$ is the unit volume gas concentration, $k$ is the Boltzmann constant, and $T$ is the absolute temperature.

From Eqs. (1.8) and (1.9), the critical radius $R_c$ and the critical free energy barrier $W_{hom}$ have a strong dependence on the surface tension of the melt and the pressure difference inside and outside of the cell nucleus. Therefore, increasing the supersaturation degree, decreasing the polymer melt surface tension, and increasing the internal and external pressure difference are approaches to reduce the critical radius and the critical independent energy barrier, which would enhance the cell nucleation rate and the number of cells that can be formed. In addition, increasing the depressurization rate, the gas concentration, and the system temperature would also increase the cell nucleation rate. However, some conditions are contradicted naturally such as the gas concentration would be reduced when elevating the temperature. Hence, saturation pressure is usually recognized as the most influential factor in the cell nucleation rate.

#### 1.3.2.2 Heterogeneous Foam Nucleation

If there is a second phase in the system, such as foreign impurities or nucleating agents, the energy barrier for cell nucleation would be lower with the coexistence of the gas–liquid–solid three phases. The composite interface can serve as a starting point for cell nucleation in heterogeneous nucleation. The critical radius $R_c$ and free energy barriers $\Delta G$ in heterogeneous nucleation were calculated similarly to homogeneous nucleation, as shown in Eq. (1.11).

$$\Delta G = -\Delta P \cdot V_G + (\gamma_{sg} - \gamma_{sl})A_{sg} + \gamma_{lg}A_{lg} \tag{1.11}$$

where $\gamma_{sg}$ is the surface tension of the solid–gas interface, $\gamma_{sl}$ is the surface tension of the solid–liquid interface, $A_{sg}$ is the solid–gas interface surface area, and $A_{lg}$ is the liquid–gas interface surface area.

The first term in Eq. (1.11) is the work done by the volume expansion of the gas inside the cell, the second term is the energy required to replace the solid–liquid interface with the solid–gas interface, and the third term is the work required to create the liquid–gas interface that constitutes the cell. The triple-phase composite interfacial energy follows the relationship described by Young's equation (1.12).

$$\gamma_{sg} = \gamma_{sl} + \gamma_{lg}\cos\theta \tag{1.12}$$

The shape of the heterogeneous nucleating cell nucleus takes a deficient spherical shape as shown in Figure 1.3(b). The free energy barriers $\Delta G$ can be expressed as Eq. (1.13):

$$\Delta G = -\Delta P \cdot V_G + \gamma_{lg} \cdot A_{lg} - \pi r^2 \cdot \gamma_{lg} \cdot \cos\theta \tag{1.13}$$

The volume $V_g$ of the cell nucleus is:

$$V_G = \pi R^3 \frac{2 - 3\cos\theta + \cos^3\theta}{3} \tag{1.14}$$

The surface area of the cell nucleus $A_{lg}$ is:

$$A_{lg} = 2\pi R^2(1 - \cos\theta) \tag{1.15}$$

The contact surface radius is:

$$r = R\sin\theta \tag{1.16}$$

By substituting the above equations into Eq. (1.13), deriving it and making it equal to 0, the critical radius of the cell nucleus of heterogeneous nucleation can be obtained as:

$$R_c = \frac{2\sigma}{\Delta P} \tag{1.17}$$

$$\Delta G^*_{het} = W_{het} = \frac{16\pi\sigma^3_{bp}}{3\Delta p^2} S(\theta) \tag{1.18}$$

$$S(\theta) = \frac{(2+\cos\theta)(1-\cos\theta)^2}{4} \tag{1.19}$$

where $\theta$ is the wetting angle, $S(\theta)$ is the out-of-phase factor and a function of the contact angle, and $\sigma_{bp}$ is the interfacial tension of polymer–gas cells.

Colton and Suh [15] found that when the wetting angle is 20°, the free energy barrier between homogeneous nucleation and heterogeneous nucleation could be on the order of $10^{-3}$. The heterogeneous nucleation rates can be derived as follows.

$$N_{het} = f_1 C_1 \exp\left(\frac{-\Delta G^*_{het}}{kT}\right) \tag{1.20}$$

where $f_1$ is the frequency factor of heterogeneous nucleation, $N_{het}$ is the heterogeneous nucleation rate, and $C_1$ is the concentration of heterogeneous nucleation points.

Therefore, the activation energy required for heterogeneous nucleation is much lower than that required for heterogeneous nucleation, as compared in Figure 1.5.

#### 1.3.2.3 Mixed Nucleation Theory

Cell nucleation during the foaming process may take homogeneous and heterogeneous nucleation modes, but they are not mutually exclusive. Due to the relatively low activation energy required, heterogeneous nucleation is performed first in a system contains cell nucleation agent. Whereas homogeneous nucleation would also

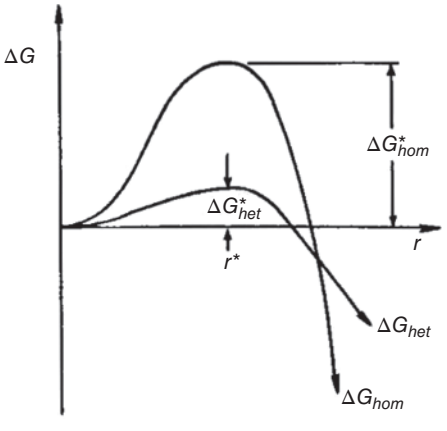


**Figure 1.5** Comparison of the free energy barrier between homogeneous nucleation and heterogeneous nucleation.
Source: Colton and Suh [15a]/with permission of John Wiley & Sons.

occur since the nucleation time is short, gas diffusion in the polymer melt system is hindered by the melt viscoelastic resistance during the heterogeneous nucleation, which would form a local supersaturation. Thus, heterogeneous nucleation followed by homogeneous nucleation would take place. The two-nucleation processes are not simply additive but rather interact with each other.

On the one hand, the first occurring heterogeneous nucleation consumes part of the gas, which makes the system supersaturated, and then the subsequent homogeneous nucleation rate drops and decreases in quantity [15a, b]; On the other hand, the internal pressure was relatively high in the cells with smaller size. When physical contact is established among these cells, the cells tend to merge, which will result in a decrease in cell density and uneven cell size. The gas concentration after heterogeneous nucleation started for time $t$ can be expressed by:

$$C' = C_0 - N_{het} \cdot t \cdot n_b \tag{1.21}$$

where $t$ is the time calculated from the occurrence of the first homogeneous nucleation, and $n_b$ is the number of gas molecules in cell nuclei.

Substituting Eq. (1.21) into Eq. (1.10) yields the rate expression for homogeneous nucleation in heterogeneous systems:

$$N'_{hom} = f_0 C' \exp\left(\frac{-\Delta G'_{hom}}{kT}\right) \tag{1.22}$$

Then, the total nucleation rate of the heterogeneous system is:

$$N = N'_{hom} + N_{het} \tag{1.23}$$

In the foaming system with a large amount of nucleation agents, the homogenous nucleation is usually ignored due to the high heterogenous nucleation rate. Moreover, besides the classical nucleation theory, new nucleation theories have been established on the basis of classical nucleation theory, such as interface nucleation theory [16], free volume theory [17], shear nucleation [18], and hot spot nucleation [19].

### 1.3.3 Cell Growth

Right after the cell nucleation, the nucleus with a radius over the critical value would start to grow into cells. The vesicular structure is mainly formed at this stage, and the size, geometric type, density, and distribution situation of the cells all have an important influence on the performance of the foam. To study the process of cell growth, the dynamics and resistance during cell growth need to be analyzed. Due to the complexity of polymer melts and the complex transfer process of mass, momentum, and heat between cells and melt components, it is difficult to accurately describe the growth process of each cell.

Cell growth kinetics can be studied in the way of theoretical simulations and experimental observations. Ramesh [20] summarized the theoretical and experimental analysis of the bubble growth model since 1917 using the prevalent single bubble growth model [21] and the cell model [22]. The single bubble

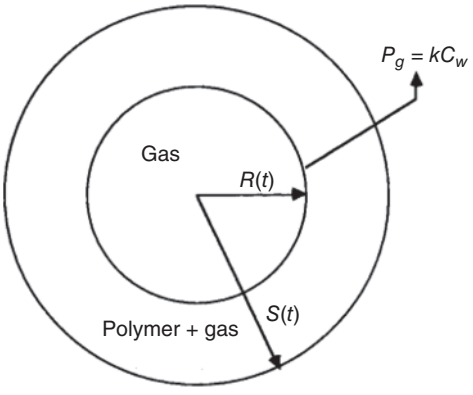


**Figure 1.6** The single bubble growth model in the foaming process. Source: Han and Yoo [21]/with permission of John Wiley & Sons.

growth model (Figure 1.6) describes the process of bubble length growth behavior of a single bubble in an infinite melt, but it has limitations in practical applications.

Cell models are roughly divided into two categories: one is a closed cell model without a blowing agent and gas loss, and the other is an extrusion foaming modified cell model with a blowing agent and gas loss, which is suitable for different application scenarios – the former is suitable for injection molding, and the latter is more suitable for extrusion molding. Based on the bubble growth kinetics of the cell model, the following equation describing the isothermal growth of cells is obtained. To analyze the cell growth process, a set of control equations needs to be solved simultaneously: the continuity of the polymer–gas solution around the cell interface, the momentum equilibrium and gas diffusion equations, the constitutive equations describing the viscoelastic properties of the polymer–gas solution, and the mass conservation equation of the gas molecules [22, 23].

$$\ddot{R}R + \frac{3}{2}\dot{R}^2 + \frac{4K(2\sqrt{3})^{n-1}}{n\rho_l}\left(\frac{\ddot{R}}{R}\right)^n = \rho_l\left(P_g - P_\infty - \frac{2\gamma_{pb}}{R}\right) \tag{1.24}$$

$$\frac{\partial C}{\partial t} + V_r\frac{\partial C}{\partial r} = \frac{D}{r^2}\frac{\partial}{\partial r}\left(r^2\frac{\partial C}{\partial r}\right) r \geq R \tag{1.25}$$

$$\frac{d}{dt}(\rho_g R^3) = 3R^2\rho_l D\left(\frac{\partial C}{\partial r}\right)_{r=R} \tag{1.26}$$

where $C$ is the gas concentration, $D$ is the diffusion rate, $P_g$ is the internal pressure of cells, $K$, $n$ is the viscoelastic characteristic parameter obtained from the power law equation $\mu = K\dot{\gamma}^{n-1}$, $P_\infty$ is the pressure at the outer boundary of polymer cells, $V_r$ is the radial velocity component $= \dot{R}R^2/r^2$, $\dot{\gamma}$ is the shear rate, and $\gamma_{pb}$ is the surface energy of the polymer–cell interface. Equation (1.24) is a continuity equation that assumes that the polymer is a non-Newtonian fluid, which can be described by the power law equation. Equation (1.25) is the gas diffusion process equation, mainly resulting from the gas concentration gradient around the gas cell. Equation (1.26) describes the gas consumption equation, mainly with the process of cell expansion at the gas melt interface. By modeling the cell growth process using numerical or finite element methods, it is possible to understand the effect of different

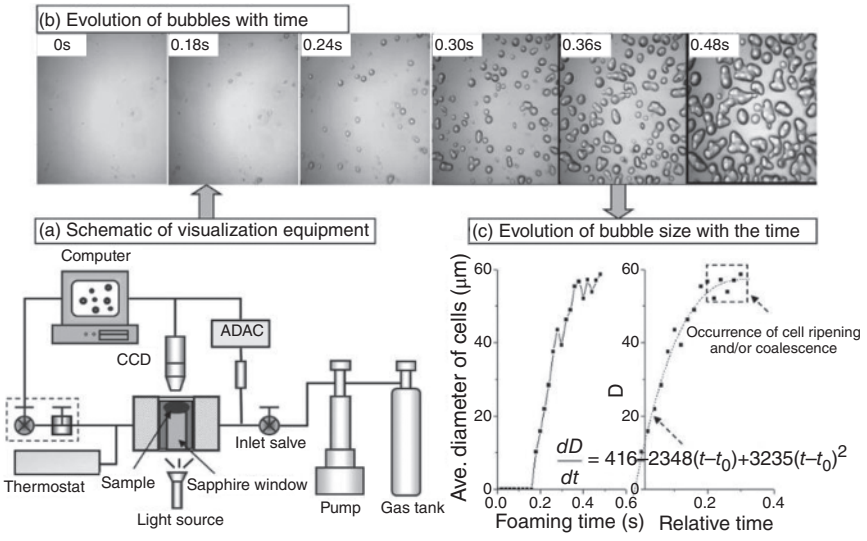


**Figure 1.7** *In situ* visualization investigating the evolution of nucleated cells. Source: Zhai et al. [24]/with permission of John Wiley & Sons.

parameters in the cell growth process and give guidance on the actual production of polymer foams.

The experimental observational study is another avenue to investigate the growth of gas cells. Using visualization techniques, it is possible to directly observe the evolution of the cellular morphology during foaming so as to verify the theoretical model and study the actual foaming process. Park et al. have made significant contributions in this field. They [24] used an *in situ* visualization technique to study the cell growth kinetics during PEO foaming, and the actual process of cell growth is shown in the following Figure 1.7. They also developed a visualization system for observing the plastic foaming process under extensional stress [25] and shear stress [26].

### 1.3.4 Cell Coalescence and Rupture

Cell coalescence is extremely easy to occur during the cell growth phase, when the cells grow into contact, the expansion tends to move toward the "weak" side, which is usually the larger cell, so coalescence and rupture usually occur successively. From the viewpoint of cell growth dynamics, cell rupture is due to the joint force between contacting cells to promote the growth of cells under the combined effect of internal and external pressure differences, surface tension, and normal stress. Thermodynamically, the surface area after cell merging is smaller, and the total free energy of the system is lower, so connecting cells tend to merge. The merging of cells can lead to uneven distribution of cells, reduced density, and poor mechanical properties of the foam. However, when the cell rupture behavior is accurately controlled, it is possible to increase the cell opening rate and alter the microstructure of the cells. Thus, the bull rupture mechanism deserves an in-depth analysis.

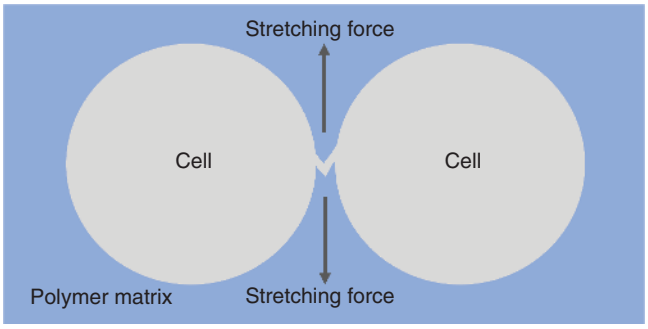


**Figure 1.8** Cell merging of adjacent cells due to the cell wall rupture.

#### 1.3.4.1 The Mechanism of Cell Rupture

During cell growth, the cell wall would be subject to a stretching force along the direction of cell growth, as illustrated in Figure 1.8. The cell wall would rupture if the stretching force is much greater than the surface tension of the melt [27]. During the foaming process, the cell size is not very uniform due to the curvature radius difference between the small and large cells and the merge of cells. The larger the size difference between adjacent cells, the greater the gas pressure difference inside them, and the more likely the small cells to merge into the large cells [28].

Cell coalescence reduces the number of cells and increases the cell size. Even if a large number of cell nuclei are formed during the nucleation stage, the cell coalescence during the cell growth process often causes a reduction in cell density. Therefore, to obtain foamed materials with high cell density and small size, it is necessary to strictly control the cell coalescence during cell growth. Cell coalescence can be suppressed by improving the melt strength of the matrix polymer and controlling process conditions. The melt strength of the polymer can be enhanced by introducing branching molecular chains, cross-linking, and blending with other polymers with higher melt strength. In terms of process control, within the temperature range at which the polymer can be foamed lowering the foaming temperature of the polymer, and increasing the cooling rate can all play a role in preventing cell coalescence [28, 29].

#### 1.3.4.2 Mechanism of Cell Opening

Foam coalescence and rupture will cause the mechanical properties of microcellular materials to decline, while in producing open-cell structure foaming materials, controllable obtaining open cell structure is sometimes necessary. Open-cell foam materials are materials in which both phases of the gas–solid phase are continuous and have a unique three-dimensional morphology, which can be further divided into fully open and partially open cell types. Due to the characteristics of reciprocal flow between the pores of the open-cell foams, such foams usually have excellent absorption and penetration properties. Open-cell foams are widely used in filtration, sound reduction, electromagnetic shielding, and biomedicine fields, especially in tissue engineering scaffolds, biological dialysis materials, etc.

So far, most open-cell foams are produced by the phase separation method or chemical foaming during material synthesis. It is challenging to produce open-cell foams via physical foaming or SCF foaming. In the phase separation (phase inversion) method, a two-phase or multiphase mixed system containing a polymer matrix and solvents is prepared, followed by triggering the phase separation process under the action of temperature or solvent to produce a cell structure within the polymer collective. It suffers from hazardous disposal of chemical solvents and residual solvents, as well as complicated procedures that usually use large amounts of water. In addition, adding water-soluble porogens into the polymer matrix is another approach to fabricating open-cell foams. Mosanenzadeh et al. [30] prepared polylactic acid (PLA) foams with high sound-absorbing properties by using salt granules as porogen, and this method was called the particle leaching technique.

Aiming at the preparation of open cell foams by SCF foaming, a large number of scholars have proposed different mechanisms and technical practices. Rodeheaver and Colton [31] proposed a theoretical model of open-cell foaming on the basis of classical foaming theory. He divided the process of cell opening into two stages, one was the collision stage, which contained the process of cell nucleation, growing up to the contact of cell walls, and the other was the stage in which the cell wall became thinner and broken into a hole. The theoretical model for the first stage is similar to the closed cell foaming process in which there must be sufficient nucleation points to guarantee that the cells grow to final contact, assuming that the number of nucleation points is equal to the number of cells eventually formed, the critical number of nucleation points required to form open cell foams can be deduced, and then the pressure versus temperature range required for foaming can be deduced. In the second stage, when the walls of the cells are in contact, by studying the kinetics of the rupture of the film, according to the Young Laplace equation and the equation of surface wave initiated by thermodynamic instability, the unstable conditions of the walls of the cells are deduced. Therefore, the time of the rupture of the cells, which is the time when the cell walls reach a critical thickness, can be estimated. According to the above model, the formula to estimate the rupture time of the cells can be derived:

$$\Delta t = \left(\frac{2\sqrt{3}A}{V}\right)\ln\left(\frac{h_0}{2\sqrt{6}A}\right) \tag{1.27}$$

$$A = \sqrt{\frac{kT}{\sigma}} \tag{1.28}$$

where $\Delta t$ is the time of cell wall rupture, $V$ is the rate of cell wall thinning, $A$ is the size of surface waves, $h_0$ is the original wall thickness, $k$ is Boltzmann constant, and $T$ is the cell wall temperature.

From the equations, it can be seen that the rupture time $\Delta t$ is a function of the cell wall thinning rate $V$, Boltzmann constant $k$, foaming temperature $T$. Rodeheaver and Colton [31] conducted a batch foaming experimental study on PS using nitrogen gas as foaming agent to verify this model, and the experimental results led to the following process conditions that enabled PS to produce open cell structures, that

is, foaming pressure was more than 17.2 MPa, foaming temperature was more than 200 °C, and foaming time was controlled between one and two seconds. Enayati et al. [32], based on this model, investigated the foaming process parameters of the PS batch foaming system by using $scCO_2$ as the foaming agent, and the experimental results proved that open-cell foams can be obtained with a minimum foaming time of six seconds at a minimum pressure of 13 MPa and a minimum temperature of 150 °C, which in general agree with the theoretical predictions.

Derrick [33] first proposed the immiscible polymer blending theory model in 1994, which is based on the principle of using immiscible two polymers to form a two-phase structure. The interface between the two phases makes it easier to form nucleation points due to the lower free energy required for nucleation, similar to the heterogeneous nucleation in classical nucleation theory. Due to the weak interaction between the two incompatible phases at the interface, the bonding between the two phases begins to detach as the cells grow, ultimately forming an open-cell structure. Yu et al. [34] prepared biodegradable polybutylene succinate (PBS)/PLA foam with open-cell structure by batch foaming owing to the small dispersion PBS phase and the relatively low melt strength of PBS compared with PLA as shown in Figure 1.9.

Lee and Park et al. [35] also prepared open-cell microcellular foam materials using an immiscible polymer blending system. They proposed two mechanisms for cell opening (Figure 1.10). One is to use polymers with higher melt strength as the continuous phase and to add a small amount of polymers with lower melt strength as the dispersed phase, which is similar to the PBS/PLA blends system. During the cell growth process, the low melt strength dispersion phase would be easily broken by the stretching force of the cell wall. Another method is to use polymers with low melt strength as the continuous phase and polymers with higher melt strength as the dispersed phase. As the cell size of the cell continues to grow, the stretching of the soft phase polymer matrix is transmitted to the hard phase polymer, and the peeling of the cell wall occurs at the junction of the two phases due to different degrees of deformation of the two phases. There are also some scholars using ultrasound-assisted techniques for the preparation of open-cell foam [36], and found that ultrasound can induce the rupture of the cell walls to form an open-cell structure.

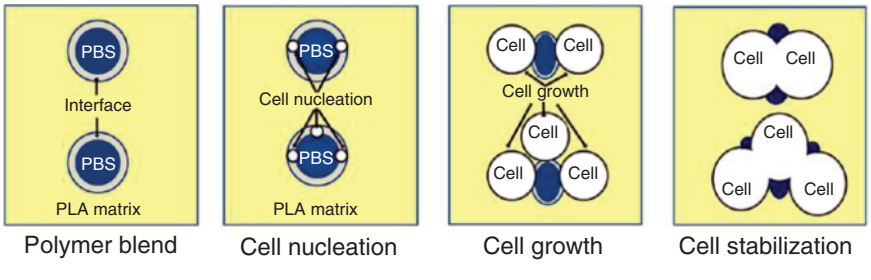


**Figure 1.9** Cell opening mechanism during the $scCO_2$ foaming of PBS/PLA blends. Source: Yu et al. [34]/with permission of American Chemical Society.

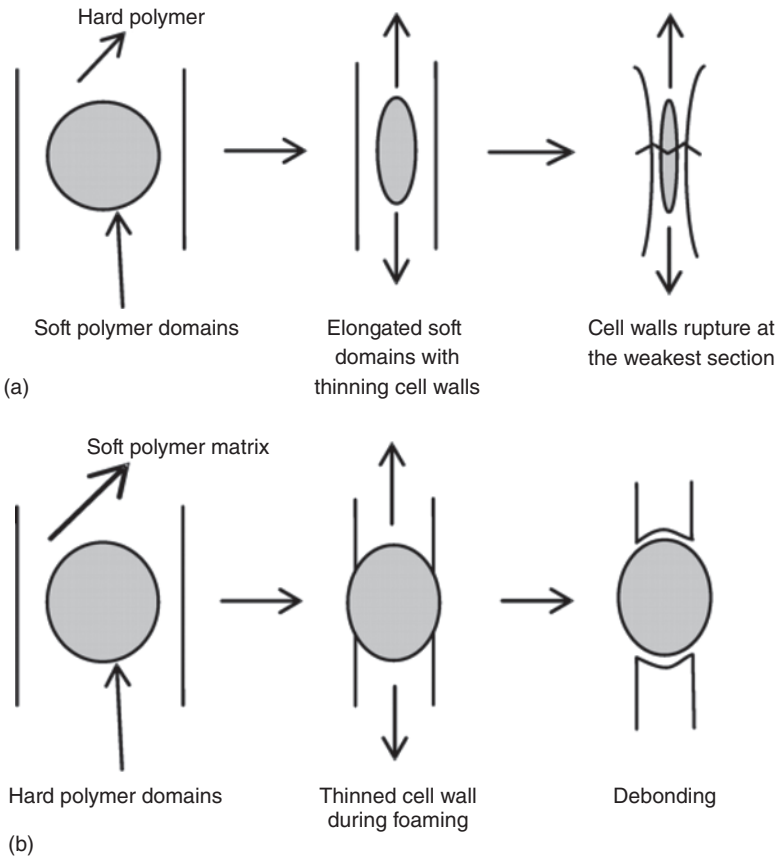


**Figure 1.10** Two cell-opening mechanisms for the system composed of (a) a high melt strength matrix phase and a low melt strength dispersion phase, and (b) a low melt strength matrix phase and a high melt strength dispersion phase. Source: Lee et al. [35b]/with permission of American Chemical Society.

### 1.3.5 Solidification and Curing

Solidification and curing, the final step in the foaming process, have an important impact on the final structure and properties of polymer foams. Since the foaming process is inherently unstable, both cell nucleation and cell growth are essential energy-dissipating processes to reestablish equilibrium. The transformation of polymers from the molten state to the solid state is a process of molecular chain mobility reduction, which enables the maintenance of the cell structure. In the case of amorphous polymers, sample cooling below the vitrification temperature allows the solidification of the cell morphology. For crystalline polymers, solidification is achieved by a sharp rise in viscosity with the crystallization of the polymer chains. For some polyurethane foams, curing is achieved by cross-linking reactions. In general, the heat is taken away by cooling the foam directly or indirectly through air, water, or other cooling media. However, polymer foams are poor conductors of heat, which

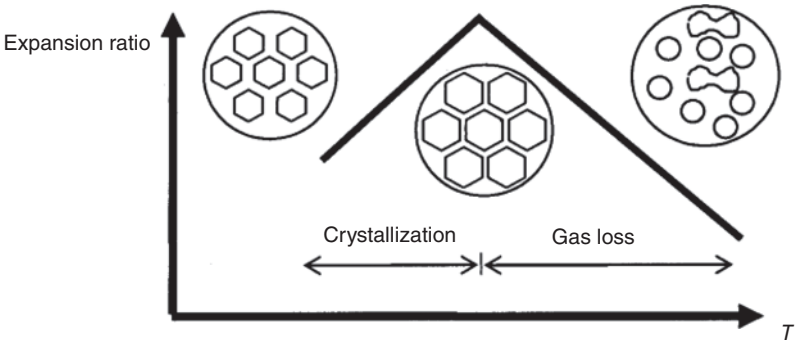


**Figure 1.11** Effect of cooling temperature on the volume expansion and cell structure of PP foam. Source: Naguib et al. [37]/with permission of John Wiley & Sons.

often causes that the cells close to the surface have been stereotyped by cooling, while the interior cells are still at a high temperature. Therefore, the outward heat transfer from the interior may cause the surface temperature to rise and destroying the cellular structure close to the surface. At the same time, the temperature difference between the inside and outside leads to the tendency of inner cells to have expansion relative to the surface layer, which will lead to stress concentration and even deformation and rupture of the cells. So, the solidification and curing process is important for the foams to maintain a stable and uniform porous structure.

Naguib et al. [37] studied the expansion behavior of PP foams and found that the final volume expansion ratio of butane as a foaming agent for extruded PP foams was related to the cooling temperature, exhibiting a trend as shown in Figure 1.11. The PP volume expansion ratio was jointly determined by the loss of the foaming agent and the crystallization of the polymer matrix. When the temperature was too high, the high diffusion rate of the foaming agent would cause the rapid loss of gas and reduce the expansion degree of the cells. When the temperature was too low, the polymer crystallized too fast, and the cells were fixed without full expansion.

## 1.4 Influencing Factors of Cell Structure in the Foaming Process

The structure of cells has a decisive influence on the performance of polymers, and the cell structure is directly related to the foaming material and the foaming parameters. The influential factors for cell structure can be roughly divided into two categories. One is the influence of physical properties of substances in the system, such as rheological properties of polymers, solubility and diffusion rate of the foaming agent in the polymer matrix, the interaction between foaming agent and polymer matrix, the influence of added nucleating agent and nanoparticles, etc. The other is the influence of foaming process parameters, such as foaming temperature, saturation pressure, depressurization rate, and depressurization method, etc.

### 1.4.1 Effects of Polymer Properties

#### 1.4.1.1 Rheological Properties of Polymers

Rheological properties of polymer matrix have an important impact on the overall foaming process. During foaming, the melt around the cells undergoes tensile action, and the rheological properties of polymers directly affect cell growth. The cell would be difficult to grow within a polymer matrix with high melt strength. When the melt strength is too low, the cells tend to rupture and collapse, resulting in a low expansion rate.

The molecular structure has a huge influence on the tensile viscosity of polymers, and the viscosity of long-chain branched polymers is higher than that of linear-chain polymers. Park and Cheung [38] found that the closed cell rate of branched PP foams in extrusion foaming was much higher than that of linear PP foams, suggesting that the cells are more easily ruptured for the low melt strength linear PP. Fang et al. [39] used γ radiation to prepare a series of long-branched PLA materials and produced a bimodal foam morphology, which verified that the introduction of long-branched structures enhanced the complex viscosity, shear thinning, and storage modulus of the matrix and improved the foaming properties of the PLA materials.

The influence of the polymer matrix crystallization behavior on the rheological properties is not negligible during the foaming process. For example, PP is a crystalline polymer that barely flows below the melting temperature due to the restriction of the crystalline regions. However, as soon as the melting temperature is reached, the viscosity and melt strength decreases sharply, which induces fast gas diffusion and cell merge during foaming, making it difficult to form a well-established cellular structure. Therefore, the melt strength of polymers is often improved from the perspective of polymer modification, and the current common methods of polymer modification mainly include crosslinking modification [40], grafting modification [41], blending modification [42], and filling with nanoparticles [43].

#### 1.4.1.2 Solubility and Diffusion of Blowing Agent

In general, the solubility of gases in molten polymers increases with increasing pressure and decreases with increasing temperature, with pressure and temperature showing opposite trends in promoting the solubility of gases in polymers (Figure 1.12). Sato et al. [44] measured the solubility of $CO_2$ and $N_2$ in molten PP and high-density polyethylene (HDPE), and the experimental data coincided with the trend of solubility change represented in Figure 1.12.

The diffusion rate of gas in a polymer matrix represents the rate of movement of gas molecules through the molten polymer, which is the mass transport capacity of gas molecules through the matrix. For large-scale production of industrial foaming products, the diffusion rate is usually a more important influencing factor. The general trend of the gas diffusion rate in the molten polymer increases with increasing temperature, quite the opposite trend of the solubility change with temperature. The decrease of surface tension is beneficial to the diffusion and mixing of substances, and the adoption of supercritical gas can reduce the surface tension of gas and polymer melts, thus, elevating the diffusion rate. Sota and Suh et al. [44, 45] studied the

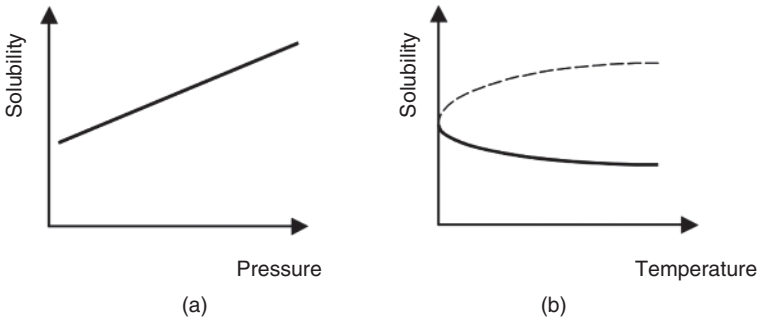


**Figure 1.12** Solubility of gas in most molten polymers: (a) solubility changes with increasing pressure, and (b) solubility changes with increasing temperature.
Source: Adapted from Xu [3a] and Cha [8].

gas diffusion theory in molten polymers to provide a basis for estimating the diffusion rates of gases. Peng and Qu [46] found that introducing a vibrational force field could promote the diffusion of small molecule gases in polymers, demonstrating that changing the external force field could elevate the diffusion rate of gases.

Controlling the diffusion direction of gas in the melt also affects the cell structure of foams, since the gas diffuses into the cell voids also diffuses to the surface and external environment. Siripurupu et al. [47] found that reducing the diffusion speed of gas to the melt surface resulted in a more dense cell structure with a smaller cell size. Mi and coworkers [48] successfully produced fine cells on the surface of the thermoplastic polyurethane (TPU) and polyvinylidene fluoride (PVDF) foamed sheets by introducing various gas barrier films to reduce the diffusion speed of $CO_2$.

#### 1.4.1.3 Interaction Between Foaming Agent and Polymer Matrix

As mentioned above, the addition of foaming agents may interact with the polymer matrix thus affecting the properties of the polymer as well as the foaming behavior. For example, $scCO_2$ has a plasticizing effect on the melt when saturated within the polymer matrix, which would improve the activity capacity of molecular chains, thus affecting the properties of the polymer matrix. For amorphous polymers, it decreases the glass transition temperature and viscosity of the polymer. For crystalline polymers, it usually affects the crystallinity, crystallization temperature, crystallization kinetics, and crystal structure. Garg et al. [49] proposed two mechanisms for the plasticizing effect of SCF addition. One is the alleviation of entanglement of polymer molecular chains after the addition of gas, and the other is the generation of additional free volume, which increases the mobility of molecular chains.

Chiou et al. [50] investigated the effect of $CO_2$ on the glass transition temperature ($T_g$) of polymers such as PMMA, PS, and polyvinyl chloride (PVC) using a high-pressure differential scanning calorimetry, and showed that $CO_2$ can significantly decrease the $T_g$ of glassy polymers with high $CO_2$ solubility at moderate pressures. The effect of $scCO_2$ on the $T_g$ of polymers can be divided into three regions, as shown in Figure 1.13. When the pressure is low (region I), the absorption of $CO_2$

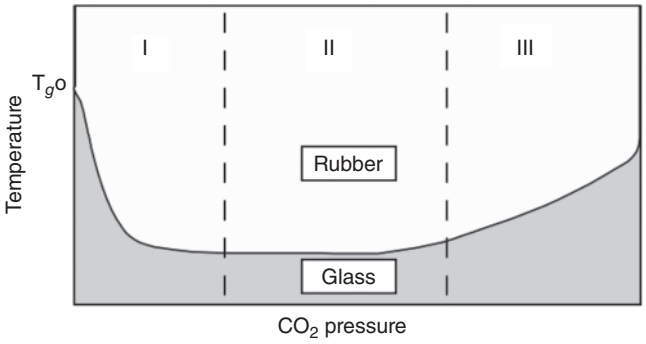


**Figure 1.13** Proposed model of glass–liquid transition for a polymer–$CO_2$ mixture. Source: Royee [51]/with permission of NC State University Libraries.

causes swelling, and the $T_g$ significantly decreases; With the increasing pressure (region II), the $T_g$ tends to stabilize and is less affected by the pressure; As the pressure further increases (region III), the free volume of the system decreases, and the $T_g$ begins to rise [51].

Zhang et al. [52] found that the presence of $scCO_2$ could significantly improve the crystallinity of PP, and the crystallinity was increased with the increase of $CO_2$ pressure. Liao et al. [53] found that the content of γ crystals increases continuously with the increase of $CO_2$ pressure in PP. Some studies found that under the influence of $CO_2$, the crystallization kinetics, and morphology of polymers such as PVDF [54], polyethylene terephthalate [54, 55], and polycarbonate [56] have also changed.

#### 1.4.1.4 Nucleating Agent and Nanoparticles

The introduction of fillers into the melt is an effective method to control the cell structure mainly due to the heterogeneous nucleation effect of the nanofillers and the effect of nanofillers on the melt strength of the matrix polymer. According to the classical nucleation theory, introducing heterogeneous nucleation can greatly reduce the nucleation barrier, thus obtaining more cell nuclei during the nucleation stage and greatly increasing the cell density. Turng [57] and Park [58] studied the effect of nanoclay on the foaming of PE, and verified the heterogeneous nucleation effect of nanoclay in improving the cell density and the performance of the foams. Antunes et al. [59] studied the effects of changing foaming parameters and introducing nano montmorillonite (MMT nanoparticles) on the PP foaming system. They found that MMT nanoparticles played a dual role in heterogeneous nucleation and improving melt strength, reducing the overall cell size and increasing the cell density.

### 1.4.2 Effects of Foaming Process Parameters

#### 1.4.2.1 Foaming Temperature

The processing temperature is an important parameter for polymer processing since the properties of a material are highly related to its temperature. In the foaming

process, temperature affects the viscosity of the polymer matrix, the solubility of the foaming agent in the molten polymer, the gas diffusion rate, and even the time needed for cooling. Foaming temperature affects the final cell morphology by influencing these physical properties.

In general, the higher the foaming temperature during the process, the lower the polymer viscosity, the lower the solubility of the foaming agent, and the faster the diffusion rate, which usually corresponds to lower cell nucleation rate, faster cell growth, lower density, and larger cell size. When the temperature is too low, and the polymer viscosity is too high, the cells would be difficult to grow. Therefore, a suitable foaming temperature window needs to be decided in the first place.

Yokoyama et al. [60] studied the foaming behavior of polystyrene (PS)/polystyrene perfluoro methyl acrylate copolymer (PFMA) blend system and obtained different cellular structures based on the change of viscosity of PS as a function of temperature. When the foaming temperature was set above the $T_g$ of PS, cells in micrometer scale were obtained; When the foaming temperature was below $T_g$ of PS, the cell size could be reduced to nano scale. Goel and Beckman [61] investigated the plasticization effect of $scCO_2$ on PMMA, and found that the solubility of $CO_2$ decreases with the increase in temperature, while the surface tension of the melt and the free energy barrier to nucleation rises with temperature increase, which leads to a decrease in the nucleation rate and the cell density.

#### 1.4.2.2 Saturation Pressure or Foaming Pressure

According to the classical nucleation theory, the pressure of the saturated gas has a great influence on cell nucleation. The higher the foaming pressure is the more gas will be absorbed by the polymer, which is responsible for a greater plasticizing effect. In addition, a high foaming pressure is usually associated with a high-pressure drop rate. All these properties are favorable for enhancing the cell nucleation rate and the cell density of the foam product, while it usually causes a decrease in cell size. Goel et al. [62] found that the size of the cells decreased with increasing pressure and the density of the cells increased with increasing pressure in the foaming of PMMA using $scCO_2$ as the foaming agent. Baldwin et al. [63] investigated the foaming process of amorphous and crystalline PET depending on the foaming pressure and found that the increasing pressure had a more significant effect on the amorphous PET than the crystalline PET. This was because high pressure could activate more homogeneous nucleation points in the amorphous PET, while the crystalline region in the crystalline PET could induce heterogeneous nucleation which will cause a high cell density even without the increase in foaming pressure.

#### 1.4.2.3 Depressurization Rate

In physical foaming with high-pressure gases, the cell nucleation and growth are generally achieved by rapid depressurization. Since cell nucleation and growth occur almost simultaneously in the system, there is clearly a competitive relationship between them. The final cell morphology is largely determined by the two processes. In the moment of pressure release, the cell nucleus started to appear in the region with a lower free energy barrier, and subsequently, more gas molecules

diffused into the cell nucleus to cause the cell growth. At a low depressurization rate, the sudden pressure drop was small, which is adverse for cell nucleation, and the time for cell growth is prolonged. Thus, more gas could diffuse into the cell nucleus forming a structure with a large cell size. On the contrary, a high depressurization rate usually refers to high cell density and relatively small cell size. Han et al. [64] studied the continuous extrusion foaming behavior of PS and adjusted the depressurization rate by changing the shape of the die. They basically found a similar tendency and prepared PS foams with different cell structures by varying the depressurization rate. Park et al. [65] designed three nozzles that can generate different depressurization rates in injection foaming to study the effect of depressurization rate on the gas competition between cell nucleation and cell growth processes. They predicted that there would be a maximum depressurization rate to enable high cell nucleation and balance the cell growth processes.

#### 1.4.2.4 Multistage Saturation and Depressurization

In most cases, the high pressure is released in one step in the foaming process. However, the pressure could also be released step-by-step in batch foaming, which is capable of controlling the cell morphology of the final foams. Step-by-step depressurization refers to the step-by-step removal of saturated pressure after supersaturation. Similarly, the foaming temperature and supersaturation pressure could also be programed stepwise to influence the final cellular structure of the foam. Typically, a bimodal cellular morphology with distinct different cell sizes in a single foam can be obtained by these multistage foaming processes since the conventional continuous nucleation and growth process is divided into two or more stages.

The foams with a bimodal cell structure that combines large cells and small cells may have advantages in their properties. The large cells could contribute to the weight reduction and the small cells could provide particular performance. Compared with the conventional singular cell structure, the bimodal cell structure may render the foams better performance in sound absorption, heat insulation, bio-tissue engineering, and other fields. Arora et al. [66] fabricated PS foams with a bimodal cell structure using a two-step depressurization method. Bao et al. [67] studied the factors affecting the bimodal cell structure in the two-step pressure drop method. They proposed that "Holding time," the duration after the first pressure drop, is important for the control of the bimodal cell structure since it controls the time for the growth of the large cells. Mi and coworkers [68] developed a multistage soaking approach in which the saturation temperature was elevated during the soaking stage to cause the precipitation of $scCO_2$ in the PLA matrix due to the lower gas solubility at higher temperatures. The precipitated $scCO_2$ formed the large cells in the subsequent depressurization step, and the prepared bimodal foams have a dramatic difference between the large cells and the small cells.

## 1.5 Previlant Foaming Methods for Microcellular Foams

Foams with cell size in the micrometer level are called microcellular foams. Compared to conventional microporous foams, microcellular foams have superior

mechanical, absorption, and insulation properties. Thus, they are been heavily investigated in recent years. Microcellular foams prepared by SCF-based foaming methods are highly recognized since the SCF are environmentally friendly and will cause no chemical residual in the polymer matrix and no VOCs emission. It also has high productivity and fabrication reliability. In a typical SCF-foaming process, SCF is first injected into the polymer to form a gas-saturated system, then the system is supersaturated by means of rapid pressure drop, which induces cell nucleation and growth, and finally, the foam with microcellular structure is cooled and solidified. SCF foaming process is mainly divided into batch foaming, continuous extrusion foaming, and injection foaming.

### 1.5.1 Batch Foaming

Batch foaming was the earliest method used to manufacture microcellular foams. The first patent for microcellular foaming was disclosed in the United States in 1984 [69]. Two batch foaming methods are widely used in practice. The first is temperature-induced foaming, in which the cell nucleation and growth are triggered by the fast temperature rising as illustrated in Figure 1.14. In this method, solid polymer preform is put in a high-pressure vessel charged with $scCO_2$ or $scN_2$ at a low temperature to form a saturated homogeneous system. Then, the saturated preform is taken out from the vessel and rapidly transferred to a hot media (i.e. hot oven and hot bath) to quickly increase the temperature above the $T_g$ of the polymer while below the melting point ($T_m$) of it. Thus, cell nucleation and growth will be triggered due to the increase in molecular chain

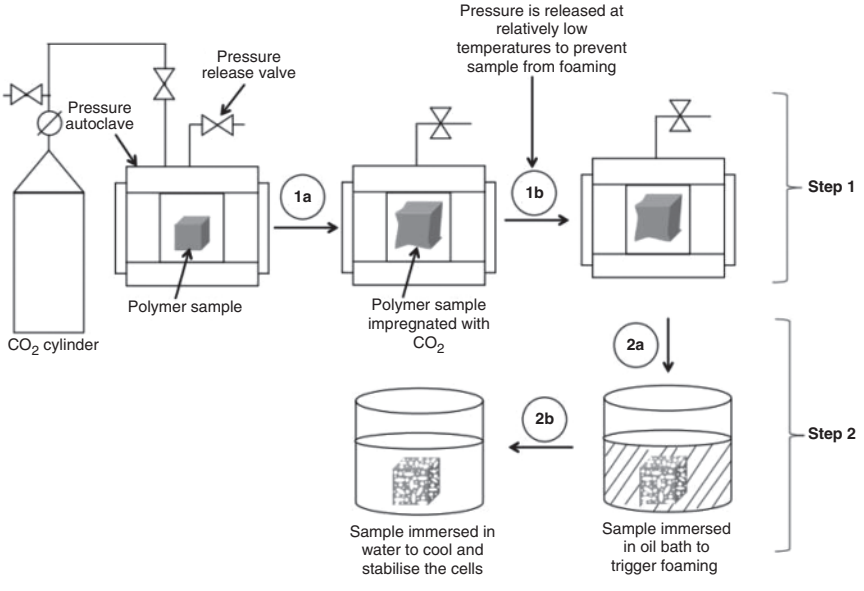


**Figure 1.14** Temperature-induced batch foaming process. Source: Okolieocha et al. [70]/with permission of Elsevier.

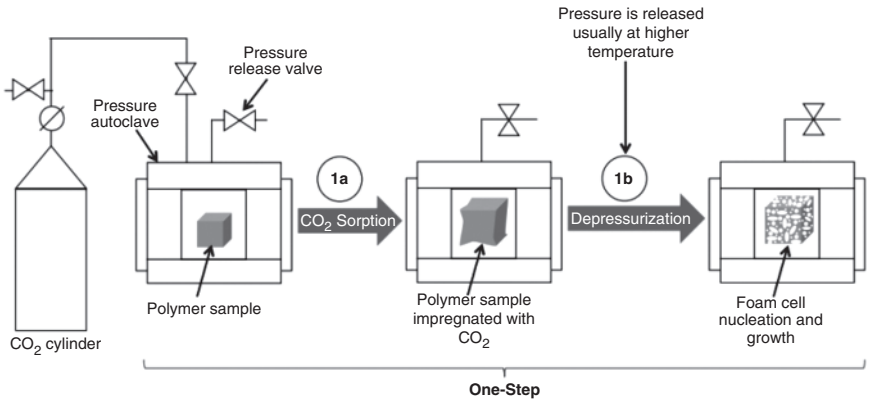


**Figure 1.15** Pressure-induced batch foaming process. Source: Okolieocha et al. [70]/with permission of Elsevier.

mobility. Finally, after the expansion process, the temperature will be reduced and the foams will be solidified by quenching. Since the samples need to be transferred from a high-pressure environment to a high-temperature environment to allow the foaming process, this method is also referred to as a two-step foaming method.

The second batch foaming method, which is used more often in practice, is called one-step foaming approach. As illustrated in Figure 1.15, in the pressure-induced foaming process, the preform samples are saturated at a higher temperature that is usually the foaming temperature with the SCF. The cell nucleation and cell growth are triggered by the rapid depressurization. Then, the expanded samples would be subject to a cooling process to allow the maintaining of the foamed cellular structures [62a].

Batch foaming method has the advantages of simplicity in foaming device, easy control of the foaming process, and easy regulation of product cell structure. However, the batch foaming method is difficult to achieve continuous production in large quantities. Batch foaming has been mainly used in laboratory research on a small scale for decades, while it is now more and more used in the industrial production of foam products attributing to the invention of novel large-scale batch foaming instruments.

### 1.5.2 Continuous Extrusion Foaming

Continuous extrusion foaming of microcellular plastics was issued in 1990s [71], which realized the continuous foaming process and promoted the industrial application of microcellular foamed products. In industry, foam extrusion lines are usually in tandem (as shown in Figure 1.16), and simple foam extrusion single line is also used in practice. In a typical extrusion foaming process, the polymer is added through the feed hopper into the extruder, it is compressed and plasticized by the screw in the first barrel and mixed with $scCO_2$ injected into the barrel to form a homogeneous system under the action of high temperature, high pressure,

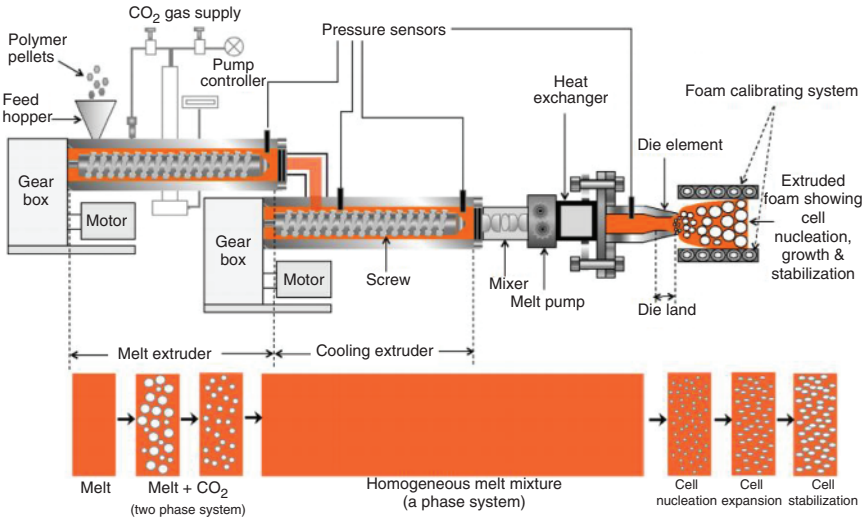


**Figure 1.16** Schematic representation of foam extrusion on a tandem line. Source: Okolieocha et al. [70]/with permission of Elsevier.

and screw shear. Subsequently, the mixed system is transferred to the second barrel where preliminary cooling takes place and higher pressure continues to increase gas concentration and saturation pressures. A static mixer, a melt pump, and a heat exchanger are sometimes used between the barrel and the die to further increase the homogeneousness and the pressure of the polymer/gas system before the extruding. Finally, as the melt passes through the die, the cell nucleation and cell growth take place rapidly due to the rapid pressure drop. Continuous extrusion foaming greatly improves production efficiency and is a key step toward the commercialization of microcellular foamed products. It has been widely used in the production of foamed sheets, plates, pipes, and beads. However, due to the restriction of die geometry, continuous extrusion foaming has significant limitations in the production of foamed products with complex shapes.

### 1.5.3 Injection Foaming Technique

In 1995, Axiomatics (later Trexel) began to develop microcellular injection molding technology based on extrusion technology and registered MuCell® [3a], the trademark most commonly used for microcellular molding technology, which is also called injection foaming or foam injection molding. Figure 1.17 shows the basic process of the injection foaming method. Similar to extrusion foaming, the polymer was added into the barrel through the funnel, and it becomes a melt under the compression and plasticization of the screw. To the melt, a defined amount of SCF was injected via a precisely controlled valve and mixed with the polymer melt by the rotation of the screw. When the polymer/gas system is plasticized and metered in front of the screw, a high-pressure state is still maintained to prevent early foaming. Subsequently, the melt is injected into the cavity of the mold, and

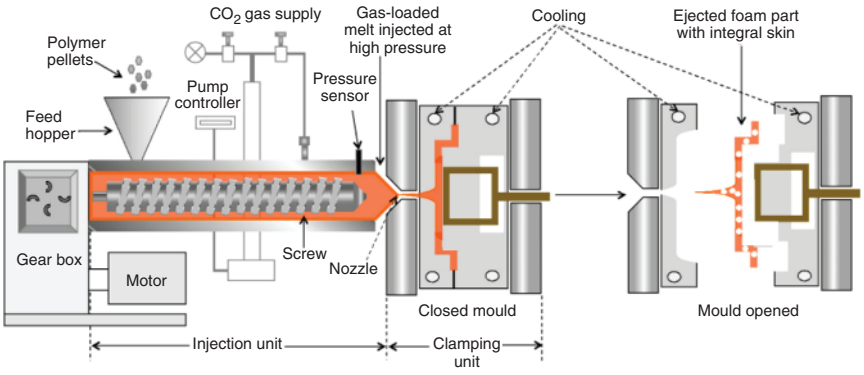


**Figure 1.17** Schematic representation of foam injection molding process. Source: Okolieocha et al. [70]/with permission of Elsevier.

the melt starts to foam as the melt fills the mold cavity due to the rapid pressure drop. For injection foaming, the holding stage is removed to allow sufficient expansion of the foamed part during the cooling cycle to achieve high weight reduction. Since the injection foaming contains plasticizing, storage, injection, and cooling stages, the cell structure of injection foamed parts is affected by various parameters, including processing temperature, injection speed, injection pressure, injection volume, mold cavity geometry, back pressure, cooling temperature, cooling time, gas content, gas injection time, *L/D* ratio of the screw, etc. In general, injection foaming improves the productivity of foamed parts and allows the production of products with complex shapes. Compared with traditional injection molding, foam injection molding has the advantages of more stable dimensions, shorter foaming cycles, and material savings. However, the high cost of the SCF supply system, the flow marks left on the surface of the foamed parts, and the quality fluctuation in production are the main concerns for this technique.

## 1.6 Advanced Applications of Functionalized Polymer Foams

With the fast development of polymer-foaming techniques and foamed products in recent years, more and more attention has been attracted. Researchers and pioneers have been devoted to exploring the advanced applications of polymer foams and trying to develop various functionalized polymer foams in the advanced fields in the new era as cutting-edge techniques. This book will focus on the advanced polymer foams that are used in cutting-edge fields. The approach to developing such foams will be mainly focused on microcellular foaming using SCF as the physical foaming agent so as to promote the potential applicability of this green technique. The content of this book will cover novel applications of the foams, including energy absorption, acoustic absorption, superhydrophobic,

electromagnetic interference (EMI) shielding, tissue engineering scaffold, flexible sensors, triboelectric nanogenerator (TENG), and solar steam generation. A brief introduction to these advanced fields and the role or potential role of polymer foams in these fields is given below.

### 1.6.1 Energy Absorbing Buffer Foam

Foam materials have a long history of applications in energy absorption and cushioning. They have found use in various industries, ranging from sports equipment like exercise pads for gymnastics, high jump, and combat, to safety products like cycling helmets and bulletproof vests. Polymer foams offer several advantages over metallic or inorganic foams. They provide greater design flexibility, are easier to process and recycle, and offer a wide range of compressive strengths, from highly elastic to semi-rigid and rigid. In addition, polymer foams are lightweight, cost-effective, easy to shape, and offer numerous advantages in commercial applications. The mechanism of energy absorption, the factors influencing the energy absorption property of polymer foams, as well as the advanced fabrication approaches of energy-absorbing polymer foams will be covered in Chapter 2.

### 1.6.2 Thermal Insulation Polymer Foams

Heat transfer occurs through three fundamental mechanisms, namely, conduction, convection, and radiation. Insulation materials are designed to impede heat transfer by reducing its occurrence through these channels. The effectiveness of insulation is determined by the material's thermal conductivity, with lower values indicating better insulation properties. Polymer foams utilize a unique cellular structure to simultaneously obstruct thermal conduction and convection processes. Their porous structure creates multiple internal interfaces, significantly enhancing their ability to block thermal radiation. Attributing to the lightweight, high surface area, and low thermal conductivity of the polymer foams, they have become essential in various applications. In Chapter 3, the thermal insulation mechanism of polymer foams, the structural design, influential factors, and the methods of fabricating advanced thermal insulation foams will be covered.

### 1.6.3 Acoustic Absorption Polymer Foams

Noise pollution is a major concern in both industrial settings and daily life, with long-term exposure negatively affecting mental and physical health. Porous materials, featuring interconnected pores that allow sound waves to enter and reflect within the material, excel at absorbing sound energy. Polymer foams, with their intricate microporous structures, provide effective sound absorption due to their ability to distort and scatter incident and reflected sound waves. Consequently, various polymer foams, such as melamine foam, PS foam, polyurethane foam, and their composites, find wide application in buildings, automobiles, ships, and aircraft for

sound absorption. The sound absorption mechanism of polymer foams, the critical influencing factors, the measurement approach, and the fabrication methods of sound absorption foams will be covered in Chapter 4.

### 1.6.4 Superhydrophobic Polymer Foams

Superhydrophobicity, observed in nature on surfaces like lotus leaves and water striders, relies on low surface energy and multilevel surface roughness. By mimicking these features through bionanotechnology, polymer foams can be transformed into superhydrophobic materials suitable for various applications, including anti-fouling, self-cleaning, selective oil absorption, and oil–water separation. The three-dimensional porous structure of polymer foams, both internally and on the surface, enhances their roughness, robustness, and stability compared to surface-engineered materials. In Chapter 5, the surperwetting theory, the chemical and structural design for superhydrophobic surfaces and foams, the methods to fabricate superhydrophobic polymer foams, and their advanced applications will be introduced.

### 1.6.5 Electromagnetic Shielding Conductive Polymer Foam

Electromagnetic shielding technology is vital for countering EMI and radiation and ensuring information security in our technology-driven world. CPFs possess multiple conductive interfaces within the micro-cell structure, which increases electromagnetic wave reflection and scattering, extending their transmission path and enhancing electromagnetic wave attenuation. Thus, the CPFs have natural advantages in EMI shielding and excellent EM wave absorption properties. The EMI shielding mechanisms for CPFs, the effect of CPF material composition and porous structure, the performance characterization methods, and the advanced approaches to fabricate CPFs will be introduced in Chapter 6.

### 1.6.6 Medical Tissue Engineering Repair

Organ and tissue transplantation faces a significant supply–demand gap, prompting the exploration of the tissue engineering field. Tissue engineering involves creating three-dimensional structures with cells and biomaterials. Due to their adjustable highly porous structure, tunable mechanical properties and surface chemistry, and biocompatible and biodegradable properties, polymer foams have been recognized as promising candidate materials for tissue repair and artificial organs. Porous polymer scaffolds have been used in the repair of various tissues, including bone, cartilage, skin, vascular, and neural tissues. In Chapter 7, the tissue engineering process, basic requirements for tissue engineering scaffolds, the property evaluation methods, and fabrication methods of tissue engineering scaffolds will be covered.

### 1.6.7 Flexible Sensors Based on Porous Polymer Foams

In the era of the Fourth Industrial Revolution, there is a growing demand for lightweight, flexible, highly sensitive sensors with fast response times. Porous polymer foams, with a lightweight nature and adjustable mechanical properties, are promising candidates for flexible pressure sensors. These materials can be customized to control piezoresistance and sensitivity by regulating cell microstructure, surface microstructure, and conductive nanofiller networks. Their versatility enables applications in health monitoring, mechanical analysis, robotic tactile perception, and more. The piezoresistive sensing mechanism, the microstructure design, the criteria of pressure sensors, and the advanced fabrication approaches will be introduced in Chapter 8.

### 1.6.8 Triboelectric Nanogenerator Based on Polymer Foams

Micro/nano energy has gained prominence with the rise of mobile electronics and microdevices. TENGs offer a novel approach to converting mechanical energy into electrical energy by making use of the electrostatic charges generated on different triboelectric materials. Polymer foams have shown promising potential to be used as a new class of friction materials for TENGs due to their rough surface, high surface area, flexibility, abrasion resistance, and low cost. In addition, their internal porous structure enhances charge generation capacity and charge density during TENG operation, making them an attractive choice for sustainable and scalable energy generation. In Chapter 9, the classification and mechanism of TENGs, the prominent factors influencing TENG performance, the advantages of polymer foams in TENG, and advanced achievements in polymer foam-based TENGs will be covered.

### 1.6.9 Porous Polymers for Solar Steam Generation

Solar steam generation is a crucial technology for addressing water scarcity and seawater desalination. Porous polymers play a vital role in enhancing solar-to-steam conversion efficiency because their highly porous structure facilitates water transport, their lightweight makes them able to float on water, and their light scattering and absorption properties render them high energy conversion efficiency. The fundamental basis of solar steam generation, the effects of porous structure and the surface properties on the solar-thermal energy conversion efficiency, the methods to characterize the solar steam generation performance, and the different types of porous polymers based solar steam generators will be covered in Chapter 10.

## References

1 Gibson, L.J. and Ashby, M.F. (1997). *Cellular Solids: Structure and Properties*. Cambridge University Press.
2 (a) Martini, J., Waldman, F., and Suh, N.P. (1982), The production and analysis of microcellular thermoplastic foams. SPE Technical Papers, Vol. 28, p. 674;

(b) Martini, J.E. (1981). The production and analysis of microcellular foam. MS Thesis, Massachusetts Institute of Technology.

3 (a) Xu, J. (2011). *Microcellular Injection Molding*. John Wiley & Sons. (b) Park, C.B., Behravesh, A.H., and Venter, R.D. (1998). Low density microcellular foam processing in extrusion using $CO_2$. *Polymer Engineering & Science* 38 (11): 1812–1823.

4 Sun, X., Liu, H., Li, G. et al. (2004). Investigation on the cell nucleation and cell growth in microcellular foaming by means of temperature quenching. *Journal of Applied Polymer Science* 93 (1): 163–171.

5 Nalawade, S.P., Picchioni, F., and Janssen, L. (2006). Supercritical carbon dioxide as a green solvent for processing polymer melts: processing aspects and applications. *Progress in Polymer Science* 31 (1): 19–43.

6 Zhai, W., Jiang, J., and Park, C.B. (2022). A review on physical foaming of thermoplastic and vulcanized elastomers. *Polymer Reviews* 62 (1): 95–141.

7 (a) Wood, C., Butler, R., Hebb, A. et al. (2002). Synthesis and processing of porous polymers using supercritical carbon dioxide. *Progress in Rubber, Plastics and Recycling Technology* 18 (4): 247–258. (b) Tomasko, D.L., Li, H., Liu, D. et al. (2003). A review of $CO_2$ applications in the processing of polymers. *Industrial & Engineering Chemistry Research* 42 (25): 6431–6456.

8 Cha, S.W. (1994). *A Microcellular Foaming/Forming Process Performed at Ambient Temperature and a Super-Microcelluar Foaming Process*. Massachusetts Institute of Technology.

9 Lee, S.-T. and Ramesh, N.S. (2004). *Polymeric Foams: Mechanisms and Materials*. CRC Press.

10 Merrill, E.W. (1996). I. States of polymers II. *Polymer Devolatilization* 33: 13.

11 (a) Suh, N.P. (2003). Impact of microcellular plastics on industrial practice and academic research. *Macromolecular Symposia*, Wiley Online Library 201: 187–202. (b) Shieh, Y.T., Su, J.H., Manivannan, G. et al. (1996). Interaction of supercritical carbon dioxide with polymers. I. Crystalline polymers. *Journal of Applied Polymer Science* 59 (4): 695–705.

12 (a) Colton, J. (1989). The nucleation of microcellular foams in semi crystalline thermoplastics*. *Materials and Manufacturing Processes* 4 (2): 253–262. (b) Durrill, P.L. and Griskey, R.G. (1966). Diffusion and solution of gases in thermally softened or molten polymers: Part I. Development of technique and determination of data. *AIChE Journal* 12 (6): 1147–1151.

13 Naguib, H.E., Park, C.B., and Song, S.-W. (2005). Effect of supercritical gas on crystallization of linear and branched polypropylene resins with foaming additives. *Industrial & Engineering Chemistry Research* 44 (17): 6685–6691.

14 Park, C.B. (2006). *Polymeric Foams: Science and Technology*. CRC Press.

15 (a) Colton, J. and Suh, N. (1987). The nucleation of microcellular thermoplastic foam with additives: Part I: Theoretical considerations. *Polymer Engineering & Science* 27 (7): 485–492. (b) Colton, J. and Suh, N. (1987). The nucleation of microcellular thermoplastic foam with additives: Part II: Experimental results and discussion. *Polymer Engineering & Science* 27 (7): 493–499. (c) Colton, J.S.

and Suh, N.P. (1987). Nucleation of microcellular foam: theory and practice. *Polymer Engineering & Science* 27 (7): 500–503.

**16** (a) Matuana, L.M., Park, C.B., and Balatinecz, J.J. (1997). Processing and cell morphology relationships for microcellular foamed PVC/wood-fiber composites. *Polymer Engineering & Science* 37 (7): 1137–1147. (b) Matuana, L.M., Park, C.B., and Balatinecz, J.J. (1998). Cell morphology and property relationships of microcellular foamed pvc/wood-fiber composites. *Polymer Engineering & Science* 38 (11): 1862–1872.

**17** Hall, P. and Stoeckli, H. (1969). Adsorption of nitrogen, n-butane and neo-pentane on chloro-hydrocarbon polymers. *Transactions of the Faraday Society* 65: 3334–3340.

**18** (a) Deshpande, N.S. and Barigou, M. (1999). Performance characteristics of novel mechanical foam breakers in a stirred tank reactor. *Journal of Chemical Technology & Biotechnology* 74 (10): 979–987. (b) Djelveh, G., Gros, J., and Cornet, J. (1998). Foaming process analysis for a stirred column with a narrow annular region. *Chemical Engineering Science* 53 (17): 3157–3160.

**19** Hansen, R.H. and Martin, W.M. (1964). Novel methods for the production of foamed polymers. Nucleation of dissolved gas by localized hot spots. *Industrial & Engineering Chemistry Product Research and Development* 3 (2): 137–141.

**20** Lee, S.-T. and Park, C.B. (2014). *Foam Extrusion: Principles and Practice*. CRC Press.

**21** Han, C.D. and Yoo, H.J. (1981). Studies on structural foam processing. IV. Bubble growth during mold filling. *Polymer Engineering & Science* 21 (9): 518–533.

**22** Ramesh, N., Rasmussen, D.H., and Campbell, G.A. (1991). Numerical and experimental studies of bubble growth during the microcellular foaming process. *Polymer Engineering & Science* 31 (23): 1657–1664.

**23** Koopmans, R.J., den Doelder, J.C., and Paquet, A.N. (2000). Modeling foam growth in thermoplastics. *Advanced Materials* 12 (23): 1873–1880.

**24** Zhai, W., Wang, J., Chen, N. et al. (2012). The orientation of carbon nanotubes in poly (ethylene-co-octene) microcellular foaming and its suppression effect on cell coalescence. *Polymer Engineering & Science* 52 (10): 2078–2089.

**25** Wong, A., Chu, R.K., Leung, S.N. et al. (2011). A batch foaming visualization system with extensional stress-inducing ability. *Chemical Engineering Science* 66 (1): 55–63.

**26** Wong, A. and Park, C. (2012). A visualization system for observing plastic foaming processes under shear stress. *Polymer Testing* 31 (3): 417–424.

**27** Baldwin, D.F., Park, C.B., and Suh, N.P. (1996). An extrusion system for the processing of microcellular polymer sheets: shaping and cell growth control. *Polymer Engineering & Science* 36 (10): 1425–1435.

**28** (a) Taki, K., Tabata, K., Kihara, S.-i., and Ohshima, M. (2006). Bubble coalescence in foaming process of polymers. *Polymer Engineering & Science* 46 (5): 680–690. (b) Zhai, W., Wang, H., Yu, J. et al. (2008). Cell coalescence suppressed by crosslinking structure in polypropylene microcellular foaming. *Polymer Engineering & Science* 48 (7): 1312–1321.

**29** Park, C.B., Behravesh, A.H., and Venter, R.D. (1997). *A Strategy for the Suppression of Cell Coalescence in the Extrusion of Microcellular High-Impact Polystyrene Foams*. ACS Publications.

**30** Mosanenzadeh, S.G., Naguib, H.E., Park, C.B., and Atalla, N. (2014). Development of polylactide open-cell foams with bimodal structure for high-acoustic absorption. *Journal of Applied Polymer Science* 131 (7): 39518.

**31** Rodeheaver, B.A. and Colton, J. (2001). Open-celled microcellular thermoplastic foam. *Polymer Engineering & Science* 41 (3): 380–400.

**32** Enayati, M., Famili, M.H.N., and Janani, H. (2013). Open-celled microcellular foaming and the formation of cellular structure by a theoretical pattern in polystyrene. *Iranian Polymer Journal* 22: 417–428.

**33** Derrick, T. (Derrick Edward)(1994). *Processing and Analysis of Microcellular Open-Cell Foams*. Massachusetts Institute of Technology.

**34** Yu, P., Mi, H.-Y., Huang, A. et al. (2015). Effect of poly (butylenes succinate) on poly (lactic acid) foaming behavior: formation of open cell structure. *Industrial & Engineering Chemistry Research* 54 (23): 6199–6207.

**35** (a) Park, C.B., Padareva, V., Lee, P.C., and Naguib, H.E. (2005). Extruded open-celled LDPE-based foams using non-homogeneous melt structure. *Journal of Polymer Engineering* 25 (3): 239–260. (b) Lee, P.C., Wang, J., and Park, C.B. (2006). Extruded open-cell foams using two semicrystalline polymers with different crystallization temperatures. *Industrial & Engineering Chemistry Research* 45 (1): 175–181.

**36** (a) Gandhi, A., Asija, N., Gaur, K.K. et al. (2013). Ultrasound assisted cyclic solid-state foaming for fabricating ultra-low density porous acrylonitrile–butadiene–styrene foams. *Materials Letters* 94: 76–78. (b) Guo, G., Ma, Q., Zhao, B., and Zhang, D. (2013). Ultrasound-assisted permeability improvement and acoustic characterization for solid-state fabricated PLA foams. *Ultrasonics Sonochemistry* 20 (1): 137–143.

**37** Naguib, H.E., Park, C.B., and Reichelt, N. (2004). Fundamental foaming mechanisms governing the volume expansion of extruded polypropylene foams. *Journal of Applied Polymer Science* 91 (4): 2661–2668.

**38** Park, C.B. and Cheung, L.K. (1997). A study of cell nucleation in the extrusion of polypropylene foams. *Polymer Engineering & Science* 37 (1): 1–10.

**39** Fang, H., Zhang, Y., Bai, J. et al. (2013). Bimodal architecture and rheological and foaming properties for gamma-irradiated long-chain branched polylactides. *RSC Advances* 3 (23): 8783–8795.

**40** (a) Schulze, D., Trinkle, S., Mülhaupt, R., and Friedrich, C. (2003). Rheological evidence of modifications of polypropylene by β-irradiation. *Rheologica Acta* 42 (3): 251–258. (b) Nam, G., Yoo, J., and Lee, J. (2005). Effect of long-chain branches of polypropylene on rheological properties and foam-extrusion performances. *Journal of Applied Polymer Science* 96 (5): 1793–1800.

**41** (a) Bahreini, E., Aghamiri, S.F., Wilhelm, M., and Abbasi, M. (2018). Influence of molecular structure on the foamability of polypropylene: linear and extensional rheological fingerprint. *Journal of Cellular Plastics* 54 (3): 515–543.

(b) Xu, Z., Zhang, Z., Guan, Y. et al. (2013). Investigation of extensional rheological behaviors of polypropylene for foaming. *Journal of Cellular Plastics* 49 (4): 317–334.

**42** (a) Doroudiani, S., Park, C.B., and Kortschot, M.T. (1996). Effect of the crystallinity and morphology on the microcellular foam structure of semicrystalline polymers. *Polymer Engineering & Science* 36 (21): 2645–2662. (b) Huang, H.-X., Wang, J.-K., and Sun, X.-H. (2008). Improving of cell structure of microcellular foams based on polypropylene/high-density polyethylene blends. *Journal of Cellular Plastics* 44 (1): 69–85.

**43** (a) Guo, M.C., Heuzey, M.C., and Carreau, P.J. (2007). Cell structure and dynamic properties of injection molded polypropylene foams. *Polymer Engineering & Science* 47 (7): 1070–1081. (b) Jiang, X.-L., Bao, J.-B., Liu, T. et al. (2009). Microcellular foaming of polypropylene/clay nanocomposites with supercritical carbon dioxide. *Journal of Cellular Plastics* 45 (6): 515–538.

**44** Sato, Y., Fujiwara, K., Takikawa, T. et al. (1999). Solubilities and diffusion coefficients of carbon dioxide and nitrogen in polypropylene, high-density polyethylene, and polystyrene under high pressures and temperatures. *Fluid Phase Equilibria* 162 (1–2): 261–276.

**45** Suh, N. (1996). *Innovation in Polymer Processing* (ed. J.F. Stevenson). Cincinnati, OH: Hanser Gardner Publications.

**46** Peng, X. and Qu, J. (1999). Extrusion mixing characteristics of filled polymer system on vibration force field. *China Plastic Industry* 2: 41–43.

**47** Siripurapu, S., Coughlan, J.A., Spontak, R.J., and Khan, S.A. (2004). Surface-constrained foaming of polymer thin films with supercritical carbon dioxide. *Macromolecules* 37 (26): 9872–9879.

**48** (a) Ni, G.-L., Zhu, X., Mi, H.-Y. et al. (2021). Skinless porous films generated by supercritical $CO_2$ foaming for high-performance complementary shaped triboelectric nanogenerators and self-powered sensors. *Nano Energy* 87: 106148. (b) Wang, L., Cui, W., Mi, H.-Y. et al. (2022). Fabrication of skinless cellular poly (vinylidene fluoride) films by surface-constrained supercritical $CO_2$ foaming using elastic gas barrier layers. *The Journal of Supercritical Fluids* 184: 105562.

**49** Garg, A., Gulari, E., and Manke, C.W. (1994). Thermodynamics of polymer melts swollen with supercritical gases. *Macromolecules* 27 (20): 5643–5653.

**50** Chiou, J., Barlow, J.W., and Paul, D.R. (1985). Plasticization of glassy polymers by $CO_2$. *Journal of Applied Polymer Science* 30 (6): 2633–2642.

**51** Royee, J.R. (2000). *Supercritical Fluid Assisted Polymer Processing: Plasticization, Swelling and Rheology*. North Carolina State University.

**52** Zhang, R.-H., Li, X.-K., Cao, G.-P. et al. (2011). Improved kinetic model of crystallization for isotactic polypropylene induced by supercritical $CO_2$: introducing pressure and temperature dependence into the Avrami equation. *Industrial & Engineering Chemistry Research* 50 (18): 10509–10515.

**53** Liao, R., Yu, W., Zhou, C. et al. (2008). The formation of γ-crystal in long-chain branched polypropylene under supercritical carbon dioxide. *Journal of Polymer Science Part B: Polymer Physics* 46 (5): 441–451.

**54** Chiou, J., Barlow, J., and Paul, D. (1985). Polymer crystallization induced by sorption of $CO_2$ gas. *Journal of Applied Polymer Science* 30 (9): 3911–3924.

**55** Lambert, S. and Paulaitis, M. (1991). Crystallization of poly (ethylene terephthalate) induced by carbon dioxide sorption at elevated pressures. *The Journal of Supercritical Fluids* 4 (1): 15–23.

**56** Beckman, E. and Porter, R.S. (1987). Crystallization of bisphenol a polycarbonate induced by supercritical carbon dioxide. *Journal of Polymer Science Part B: Polymer Physics* 25 (7): 1511–1517.

**57** Lee, J., Turng, L.-S., and Kramschuster, A. (2010). The microcellular injection molding of low-density polyethylene (LDPE) composites. *Polymer-Plastics Technology and Engineering* 49 (13): 1339–1346.

**58** Lee, Y.H., Kuboki, T., Park, C.B., and Sain, M. (2011). The effects of nanoclay on the extrusion foaming of wood fiber/polyethylene nanocomposites. *Polymer Engineering & Science* 51 (5): 1014–1022.

**59** Antunes, M., Velasco, J.I., Realinho, V., and Solorzano, E. (2009). Study of the cellular structure heterogeneity and anisotropy of polypropylene and polypropylene nanocomposite foams. *Polymer Engineering & Science* 49 (12): 2400–2413.

**60** Yokoyama, B.H., Li, L., Nemoto, T., and Sugiyama, K. (2004). Tunable nanocellular polymeric monoliths using fluorinated block copolymer templates and supercritical carbon dioxide. *Advanced Materials* 16 (17): 1542–1546.

**61** Goel, S. and Beckman, E. (1993). Plasticization of poly(methyl methacrylate) (PMMA) networks by supercritical carbon dioxide. *Polymer* 34 (7): 1410–1417.

**62** (a) Goel, S.K. and Beckman, E.J. (1994). Generation of microcellular polymeric foams using supercritical carbon-dioxide. II: cell-growth and skin formation. *Polymer Engineering & Science* 34 (14): 1137–1147. (b) Goel, S.K. and Beckman, E.J. (1994). Generation of microcellular polymeric foams using supercritical carbon dioxide. II: cell growth and skin formation. *Polymer Engineering & Science* 34 (14): 1148–1156.

**63** (a) Baldwin, D.F., Park, C.B., and Suh, N.P. (1996). A microcellular processing study of poly (ethylene terephthalate) in the amorphous and semicrystalline states. Part I: microcell nucleation. *Polymer Engineering & Science* 36 (11): 1437–1445. (b) Baldwin, D.F., Park, C.B., and Suh, N.P. (1996). A microcellular processing study of poly(ethylene terephthalate) in the amorphous and semicrystalline states. Part II: cell growth and process design. *Polymer Engineering & Science* 36 (11): 1446–1453.

**64** Han, X., Koelling, K.W., Tomasko, D.L., and Lee, L.J. (2002). Continuous microcellular polystyrene foam extrusion with supercritical $CO_2$. *Polymer Engineering & Science* 42 (11): 2094–2106.

**65** Park, C.B., Baldwin, D.F., and Suh, N.P. (1995). Effect of the pressure drop rate on cell nucleation in continuous processing of microcellular polymers. *Polymer Engineering & Science* 35 (5): 432–440.

**66** Arora, K.A., Lesser, A.J., and McCarthy, T.J. (1998). Preparation and characterization of microcellular polystyrene foams processed in supercritical carbon dioxide. *Macromolecules* 31 (14): 4614–4620.

**67** (a) Bao, J.-B., Liu, T., Zhao, L., and Hu, G.-H. (2011). A two-step depressurization batch process for the formation of bi-modal cell structure polystyrene foams using $scCO_2$. *The Journal of Supercritical Fluids* 55 (3): 1104–1114. (b) Bao, J.-B., Weng, G.-S., Zhao, L. et al. (2014). Tensile and impact behavior of polystyrene microcellular foams with bi-modal cell morphology. *Journal of Cellular Plastics* 50 (4): 381–393.

**68** Huang, J.-N., Jing, X., Geng, L.-H. et al. (2015). A novel multiple soaking temperature (MST) method to prepare polylactic acid foams with bi-modal open-pore structure and their potential in tissue engineering applications. *The Journal of Supercritical Fluids* 103: 28–37.

**69** Martini-Vvedensky, J.E., Suh, N.P., and Waldman, F.A. (1984). Microcellular closed cell foams and their method of manufacture. Gloogle Patents: 1984.

**70** Okolieocha, C., Raps, D., Subramaniam, K., and Altstädt, V. (2015). Microcellular to nanocellular polymer foams: progress (2004–2015) and future directions–a review. *European Polymer Journal* 73: 500–519.

**71** Baldwin, D.F., Park, C.B., and Suh, N.P. (1998). Microcellular sheet extrusion system process design models for shaping and cell growth control. *Polymer Engineering & Science* 38 (4): 674–688.